International Journal of Nanomedicine

Dovepress
open access to scientific and medical research

Open Access Full Text Article

ORIGINAL RESEARCH

GEM-loaded magnetic albumin nanospheres modified with cetuximab for simultaneous targeting, magnetic resonance imaging, and double-targeted thermochemotherapy of pancreatic cancer cells

This article was published in the following Dove Press journal:
International Journal of Nanomedicine
30 March 2015
Number of times this article has been viewed

Ling Wang[1]
Yanli An[2]
Chenyan Yuan[3]
Hao Zhang[2]
Chen Liang[2]
Fengan Ding[2]
Qi Gao[1]
Dongsheng Zhang[4]

[1]Department of Ultrasonography, Zhong Da Hospital, Medical School, Southeast University, Nanjing, People's Republic of China; [2]Medical School, Southeast University, Nanjing, People's Republic of China; [3]Department of Clinical Laboratory, Zhong Da Hospital, Medical School, Southeast University, Nanjing, People's Republic of China; [4]Jiangsu Key Laboratory for Biomaterials and Devices, Medical School, Southeast University, Nanjing, People's Republic of China

Background: Targeted delivery is a promising strategy to improve the diagnostic imaging and therapeutic effect of cancers. In this paper, novel cetuximab (C225)-conjugated, gemcitabine (GEM)-containing magnetic albumin nanospheres (C225-GEM/MANs) were fabricated and applied as a theranostic nanocarrier to conduct simultaneous targeting, magnetic resonance imaging (MRI), and double-targeted thermochemotherapy against pancreatic cancer cells.

Methods: Fe_3O_4 nanoparticles (NPs) and GEM co-loaded albumin nanospheres (GEM/MANs) were prepared, and then C225 was further conjugated to synthesize C225-GEM/MANs. Their morphology, mean particle size, GEM encapsulation ratio, specific cell-binding ability, and thermal dynamic profiles were characterized. The effects of discriminating different EGFR-expressing pancreatic cancer cells (AsPC-1 and MIA PaCa-2) and monitoring cellular targeting effects were assessed by targeted MRI. Lastly, the antitumor efficiency of double/C225/magnetic-targeted and nontargeted thermochemotherapy was compared with chemotherapy alone using 3-(4, 5-dimethyl-2-thiazolyl)-2,5-diphenyl-2H-tetrazolium bromide (MTT) and flow cytometry (FCM) assay.

Results: When treated with targeted nanospheres, AsPC-1 cells showed a significantly less intense MRI T2 signal than MIA PaCa-2 cells, while both cells had similar signal strength when incubated with nontargeted nanospheres. T2 signal intensity was significantly lower when magnetic and C225 targeting were combined, rather than used alone. The inhibitory and apoptotic rates of each thermochemotherapy group were significantly higher than those of the chemotherapy-alone groups. Additionally, both MTT and FCM analysis verified that double-targeted thermochemotherapy had the highest targeted killing efficiency among all groups.

Conclusion: The C225-GEM/MANs can distinguish various EGFR-expressing live pancreatic cancer cells, monitor diverse cellular targeting effects using targeted MRI imaging, and efficiently mediate double-targeted thermochemotherapy against pancreatic cancer cells.

Keywords: gemcitabine, Fe_3O_4 nanoparticles, theranostic nanocarrier

Introduction

Pancreatic cancer is the fourth most common cause of death from cancer.[1] Although great progress has been made, the 5-year survival rate of people with pancreatic cancer is still less than 5%.[2] This is mainly due to a lack of effective early diagnosis and treatment. At present, gemcitabine (GEM)-based chemotherapy remains the main treatment option for pancreatic cancer, especially for patients with advanced pancreatic cancer or as adjuvant therapy after surgical resection. However, the therapeutic effect appears extremely poor. The underlying reason may lie in the short half-life of

Correspondence: Dongsheng Zhang
Jiangsu Key Laboratory for Biomaterials and Devices, Medical School, Southeast University, Dingjiaqiao Road 87, Nanjing 210009, Jiangsu Province, People's Republic of China
Tel +86 25 8327 2502
Fax +86 25 8327 2541
Email zdszds1222@163.com

GEM in vivo and undesired adverse effects on normal tissues caused by nonspecific drug delivery.[3,4] On the other hand, the efficacy of using chemotherapy alone to treat pancreatic cancer is limited. Combining treatment methods is a promising strategy for eradicating cancer. Thus, more effective diagnostic and therapeutic strategies are urgently needed to combat this deadly disease.

Nanocarriers are novel molecules that are increasingly used as drug carriers[5] for effective accumulation within tumor tissues through the enhanced permeability and retention effect.[6] Furthermore, combining imaging and therapeutic capabilities into a single nanocarrier has generated substantial attention because of the tremendous opportunity for simultaneous diagnosis and treatment of various diseases.[7–9] Among all kinds of nanocarriers, nanospheres with a mean diameter of 10–1,000 nm have been widely applied in drug delivery systems[10–12] and have shown many advantages, including enhanced structural stability, controlled release of therapeutic agents, and protection from in vivo metabolization of encapsulated drugs.[13] Nanospheres made of albumin are especially attractive because of the following features: nontoxic, nonantigenic, biodegradable, easy to prepare, reproducible, and well tolerated. Using albumin nanospheres as drug carriers to encapsulate GEM against pancreatic cancer has been reported.[14,15] Magnetic albumin nanospheres (MANs) have become particularly interesting due to their association with magnetic nanoparticles (MNPs), which are excellent theranostic candidates, capable of incorporating imaging agents together with therapeutic agents for simultaneous diagnosis and treatment. It has been reported that a MNP-based drug delivery system may not only present enhanced structural stability, tissue absorption, and guide drugs to a specific cancer lesion within the body by utilizing the external magnetic field[16] but may also have the potential to carry out magnetohyperthermia when exposed to an alternating magnetic field (AMF),[17] magnetic resonance imaging (MRI) contrast enhancement,[18] and gene therapy.[19] MANs also have the unique magnetic potential to conduct magnetic-targeted drug delivery with the aid of an external magnetic field, carry out magnetohyperthermia, or act as contrast enhancement for MRI. Recently, some studies reported designing MANs as a new generation of drug carrier for targeted drug delivery[20,21] or as a magnetohyperthermia medium for thermoablation of tumor cells.[22–24] However, little has been reported on using MANs as an MRI contrast enhancement for cancer diagnosis or constructing theranostic MANs for concurrent diagnostic MRI and magnetohyperthermia. In addition, due to their small size and large surface area, various biomolecules such as antibodies or ligands can be conjugated onto the surface of albumin nanospheres to offer active targeted diagnosis or treatment of cancers.[22,25,26]

Active targeting approach is another highly desirable treatment technique to enhance therapeutic drug efficacy and decrease possible drug-related side effects. Active targeting is based on the over- or exclusive expression of different epitopes or receptors in tumor cells and on specific physical characteristics. Two recent studies have indicated that epidermal growth factor receptor (EGFR) was detectable in more than 95% of patients with pancreatic cancer.[27,28] High levels of EGFR expression often correlate with poor response to treatment, disease progression, and poor survival.[29] Hence, EGFR receptor could be an attractive target, and targeting it represents a promising diagnostic and therapeutic strategy for pancreatic cancer. Additionally, anti-EGFR treatment has been found to add significantly to the overall survival of pancreatic cancer patients treated with GEM.[30] Cetuximab (C225), a kind of anti-EGFR monoclonal antibody (mab), approved by the US Food and Drug Administration for the treatment of patients with EGFR-positive colorectal cancer, has now been used to treat many other carcinomas containing pancreatic cancer.[31–33] Thus, we bonded C225 to the surface of nanospheres for specific targeting of the EGFR receptors expressed on the surfaces of tumor cells to induce active targeted drug and Fe_3O_4 NP co-delivery. Moreover, once C225 was attached onto the surface of MANs, active antibody-targeted drug transportation can act at the same time as the passive accumulation of drugs in tumor tissues under an external magnetic field. Such combined magnetic- and antibody-targeted (named double-targeted) anticancer drugs delivery will be a promising alternative to conventional chemotherapy due to increased drug accumulation in cancer cells, while avoiding undesirable side effects in normal cells. Meanwhile, double-targeted magnetic fluid hyperthermia (MFH) mediated by nanosized Fe_3O_4 can also occur along with double-targeted drug delivery. Herein, double-targeted delivery is an attractive choice for cancer imaging and therapy.

In our previous study,[34] we had successfully synthesized GEM-loaded MANs. Based on that, we further conjugated C225 mab onto their surface to fabricate C225-GEM/MANs. By using them as an MRI molecular probe, we effectively distinguished different EGFR-expressing AsPC-1 and MIA PaCa-2 pancreatic cell lines by targeted MRI. We also observed various targeting effects on AsPC-1 cells through changes of MRI T2 signal intensity. Furthermore, by comparing the antitumor effects of thermochemotherapy and

chemotherapy alone in different targeted ways, we confirmed that the efficiency of double-targeted thermochemotherapy against AsPC-1 pancreatic cells was the most optimal.

Materials and methods

Materials

GEM was purchased from Haosen Pharmaceutical Co, Ltd. (Jiangsu, People's Republic of China). Bovine serum albumin (BSA), dimethyl sulfoxide (DMSO), 3-(4, 5-dimethyl-2-thiazolyl)-2,5-diphenyl-2H-tetrazolium bromide (MTT), anti-EGFR mab cetuximab (C225 mab), trypsin, *N*-succinimidyl-3-(2-pyridyldithio) propionate (SPDP), and DL-dithiothreitol (DTT) were supplied by Sigma-Aldrich Co. (St Louis, MO, USA). Annexin V-FITC (fluorescein isothiocyanate) and propidium iodide (PI) kit were obtained from Key Gen Biotech (Nanjing, People's Republic of China). All other chemicals were commercially available and of analytical grade. AsPC-1 and MIA PaCa-2 human pancreatic cancer cell strains were provided by the Cell Institute of the Chinese Academy of Sciences.

Methods

Preparation of Fe_3O_4 nanoparticles, GEM-loaded MANs, and C225-GEM/MANs

According to our previous work,[35] Fe_3O_4 NPs were prepared using chemical coprecipitation and MANs loaded with GEM (GEM/MANs) were fabricated using a modified desolvation–crosslinking method.[34] C225 were then conjugated onto the surface of GEM/MANs using SPDP, a heterobifunctional crosslinker. The specific procedure involved three steps:

1) C225 (100 μL) was added dropwise into 13.7 μL SPDP, then phosphate-buffered saline (PBS) was added to adjust the mixture to 2 mL. After 30 minutes' reaction and following 48 hours dialysis using acetate buffer as the dialysis medium, C225-PDP was produced. During the reaction, 2-pyridyl disulfide (PDP) was introduced into the C225 mab by the reaction of some of its amino groups with the *N*-hydroxysuccinimide ester side of SPDP.
2) GEM-loaded MANs (0.5 mL) were dissolved in Milli-Q water (EMD Millipore, Billerica, MA, USA). The solution volume was adjusted to 2 mL and then 20 μL of SPDP was dropped in slowly. The mixture was reacted for 60 minutes at room temperature, after which PDP structures were introduced into the GEM/MANs by the reaction of some of the amino groups on the albumin nanospheres with the *N*-hydroxysuccinimide ester side of SPDP. At the end of the reaction, the mixture was washed with acetate buffer and ultracentrifuged (12,000 rpm/20 minutes) to remove excess SPDP. The precipitate (GEM/MANs-PDP) was then dispersed in acetate buffer and 15.4 mg DTT was added for another 30 minutes' reaction, after which the PDP structures of GEM/MANs-PDP were reduced by DTT to develop thiol (-SH). After repeated centrifugation (12,000 rpm/20 minutes) and purification with PBS, the final product we obtained was GEM/MANs-SH.
3) GEM/MANs-SH was resuspended in PBS and C225-PDP was added to start a reaction. After another 24 hours of continued magnetic stirring, followed by centrifugation (12,000 rpm/20 minutes) and washing (using PBS or Milli-Q water), the final products were C225-GEM/MANs. A portion of the C225-GEM/MANs was resuspended in PBS and incubated with Alexa Fluor® 488 Conjugate rabbit-anti-mouse IgG (Cell Signaling Technology, Inc., Danvers, MA, USA) for 1 hour at 37°C in the dark, and then centrifuged (12,000 rpm/5 minutes), rinsed with PBS, and collected to determine the antibody conjugation efficiency using flow cytometry (FCM) analysis to detect fluorescent percentage (BD Biosciences, San Jose, CA, USA). C225-GEM/MANs that were not incubated with Alexa Fluor® 488 Conjugate rabbit-anti-mouse IgG were used as a control.

Characterization

The samples were freeze dried and the morphology and mean particle size of C225-GEM/MANs were characterized using transmission electron microscopy (TEM; JEM-1011; JEOL, Tokyo, Japan) and Malvern Instruments (Malvern, UK).

Determination of anti-EGFR antibody on the surface of C225-GEM/MANs

To confirm whether the anti-EGFR antibody was linked to the GEM-loaded MANs, the appropriate Alexa Fluor® 488 Conjugate rabbit-anti-mouse IgG (Cell Signaling Technology, Inc.) was added to 2 μL of C225-targeted nanospheres with 0.9% BSA and allowed to react for 1 hour at 37°C. After centrifugation at 12,000 rpm for 30 minutes, the precipitate was washed three times with PBS, redispersed in 20 μL of PBS and observed under a fluorescence microscope (BX53; Olympus Corporation, Tokyo, Japan). C225-free nanospheres were used as control.

GEM encapsulation efficiency and in vitro release test

The GEM encapsulation ratio was detected by ultraviolet spectrophotometer. Nanospheres solutions were first

lyophilized to yield solid samples. The dried samples were then weighed and re-dissolved in DMSO. Fe_3O_4 NPs were removed from the solution by magnetic field-guided accumulation. The absorbance at 268 nm was measured to determine the GEM content in the solution.

$$\text{Entrapment efficiency (\%)} = \frac{\text{Amount of GEM in the nanosphere}}{\text{Quality of nanospheres}} \times 100\%$$

GEM release profiles in vitro were evaluated by dynamic dialysis test in PBS (release medium, 37°C, pH 7.0). Briefly, 15 mL samples were placed in a pretreated dialysis bag with both ends tied tightly after ultrasonication. The bag was then immersed in a beaker containing 100 mL phosphate buffer with constant stirring (150 r/minute) at 37°C. Every 30 minutes, 5 mL samples were withdrawn from the medium and the equal volume of phosphate buffer was re-added. This process lasted for 24 hours. The amount of released drug was then determined by measuring the absorbance using a UV spectrophotometer with standard calibration curves (wavelength =268 nm). The accumulative release rate of GEM over time was thus observed.

Heating test of the C225-GEM/MANs

The iron content loaded inside the C225-GEM/MANs was determined according to the phenanthroline chemical iron quantification method.[36] Magnetofluids of different concentrations were prepared by dispersing various doses of C225-GEM/MANs in 5 mL 0.9% NaCl. Different concentrations of nanospheres were then placed in a flat-bottomed cuvette in turn. There was a 5 mm distance from the bottom of the cuvette to the center of a hyperthermia coil of high-frequency electromagnetic field (SP-04C; Shenzhen Double Power Supply Technology Co., Ltd, People's Republic of China). The output frequency was 230 kHz and the output current was 30 A. It was heated for 1 hour and the temperature was measured at 5-minute intervals.

Cell culture

AsPC-1 cells with higher EGFP expression and MIA Paca2 cells with lower expression of EGFP as proved by western blot analysis[33] were obtained and cultured in Dulbecco's Modified Eagle's Medium (DMEM; Thermo Fisher Scientific, Waltham, MA, USA) supplemented with 10% fetal bovine serum (FBS), 100 units/mL penicillin, and 100 µg/mL streptomycin (Thermo Fisher Scientific) in humidified air containing 5% CO_2 at 37°C.

In vitro MRI

In order to demonstrate the feasibility of C225-GEM/MANs serving as in vitro magnetic nanoprobe, MRI experiments were performed. AsPC-1 and MIA PaCa-2 human pancreatic cancer cells were seeded separately into T25 culture plates with 5 mL fresh growth medium and incubated at 37°C (5% CO_2) overnight to bring the cells to confluence (2×10^6 cells). The growth medium was then discarded and replaced with fresh medium containing C225-GEM/MANs and GEM/MANs at the same iron concentrations and the cells were incubated at 37°C (5% CO_2) for an additional 2 hours. After that, the growth medium was removed and the cells were rinsed twice with PBS, trypsinized, centrifuged (1,000 rpm/5 minutes), rinsed again with PBS, and resuspended in 1 mL of 1% agarose (Oxoid, Basingstoke, UK) in 10 mm diameter Eppendorf tubes (Corning Incorporated, Corning, NY, USA) for MRI. One percent agarose (1 mL) without nanospheres was used as control. T2 MRI was carried out using a 7.0-Tesla animal magnetic resonance (MR) scanner (PharmaScan; Bruker Corporation, Billerica, MA, USA) with a 23 mm mouse head circular volume coil at room temperature. A T2 spin echo sequence was used for T2-weighted imaging (repetition time [TR] =2,000 ms, echo time [TE] =13,65 ms, field of view [FOV] =40×40 mm, slice thickness =1 mm, matrix =256×256), and a T2 mapping sequence was used for obtaining the T2 value (TR =3,000, 1,500, 800, 400, 200 ms, TE =11 ms, FOV =40×40 mm, slice thickness =1 mm, matrix =256×256).

In addition, different targeting effects on AsPC-1 were monitored by targeted MRI. The cells were treated in the same way as the above approach. After being incubated with nontargeted nanospheres only (nontargeted), nontargeted nanospheres under exterior magnet (single magnetic-targeted), the targeted nanospheres only (single C225-targeted), the targeted nanospheres under exterior magnet (combined magnetic- and C225-targeted) with the same iron content for 2 hours, respectively, the cells were collected and their T2-weighted images were observed. Meanwhile, their corresponding T2 values were quantified.

Cell binding and internalization of C225-GEM/MANs

AsPC-1 cells were seeded on the glass slides for 24 hours until 50%–80% confluency was reached (so that the cell density was not too high). The cells were then fixed with 4% paraformaldehyde in PBS for 15 minutes at room temperature and permeabilized using 0.1% Triton X100 in PBS for 15 minutes at room temperature. After being blocked with 1% BSA for

1 hour, the cells were treated with C225 (positive contrast), C225-conjugated nanospheres, Ab-free nanospheres, and PBS (negative contrast), respectively, at 4°C overnight. The cells were then washed three times with PBS. The appropriate Alexa Fluor® 488 Conjugate rabbit-anti-mouse IgG (Cell Signaling Technology, Inc.; dilution 1:1,000) was then applied for incubation for 1 hour at 37°C in the dark. The cells were washed another three times with PBS and incubated again with 10 μg/mL of Hoechst 33342 nuclear stain for 5 minutes at room temperature. Finally, the cells were washed three times with PBS and imaged using an immunofluorescence microscope (BX53; Olympus Corporation).

MTT-based in vitro cytotoxicity assay

The growth inhibition rate (IR) of C225-GEM/MANs on AsPC-1 cells was evaluated by MTT assay, in which double-targeted chemotherapy alone and double-targeted thermochemotherapy (chemotherapy combined with magnetohyperthermia) were compared. Firstly, AsPC-1 cells were seeded in 96-well culture plates with 6,000 cells per well and cultured for 24 hours. Then, the cells were divided into the following groups according to the targeting method and whether they had or did not have hyperthermia: 1) a negative control group (DMEM medium containing 10% FBS); 2) a GEM/MANs group with or without hyperthermia; 3) a GEM/MANs magnetic targeting group with or without hyperthermia; 4) a C225-GEM/MANs group (with antibody targeting) with or without hyperthermia; and 5) a C225-GEM/MANs with magnetic targeting (combined magnetic and antibody targeting) with or without hyperthermia. Each group had eight wells. When magnetic targeting was required, a 96-well format magnetic plate (Chemicell GmbH, Berlin, Germany) was positioned on the cell culture plates. When conduct hyperthermia was required, cells were treated with MFH for 60 minutes under a high-frequency AMF (f=230 kHz, I=30 A). After treatment management, the cells in all groups were incubated for 48 hours. Then, 20 μL MTT solution (5 mg/mL) was added to the cells in all the groups and incubated for 4 hours at 3°C. After that, 150 μL DMSO was added, the solution was mixed for 5 minutes, and the absorbance of each cell well was measured at 492 nm using a microplate reader (Model EL x800G; BioTek Instruments, Inc., Winooski, VT, USA). Each reported result was the mean of eight wells. Cell growth IR of every group's cells was calculated according to the following formula:

$$IR\% = \frac{1 - \text{optical density [OD] of experimental group}}{\text{OD of control group}} \times 100\%$$

Flow cytometry analysis for apoptosis determination

The apoptosis rate was assessed by FCM. The AsPC-1 cells were grouped and treated as described in MTT assay. The cells in every group were collected through centrifugation at 1,000 rpm for 5 minutes, followed by washing with cold PBS three times and resuspension in binding buffer (500 μL each). Then, 3.5 μL of Annexin V-FITC solution and 10 μL of PI solution were added in turn. The stained cells were incubated for 15 minutes at room temperature in the dark. Finally, the mixture was subjected to FCM analysis (BD Biosciences). All experiments were performed in triplicate.

Statistical analysis

Obtained data were analyzed using SPSS (v18.0; SPSS Inc., Chicago, IL, USA). The statistical significance of differences in mean values between the groups was analyzed using one-way analysis of variance (ANOVA). A probability level of $P<0.05$ was considered to be statistically significant.

Results

Characterization of the C225-GEM/MANs

TEM micrographs in Figure 1A show that the prepared C225-GEM/MANs were approximately spherical and uniform with good dispersibility. Fe_3O_4 NPs were also simultaneously well incorporated into the core of the composite nanospheres. The size distribution of the composite nanospheres is depicted by the curve shown in Figure 1B. The mean hydrodynamic diameter of the C225-GEM/MANs was about 200 nm.

Determination of Ab conjugation and conjugation efficiency

After being incubated with the rabbit-anti-mouse second antibody and centrifuged, the nanospheres aggregated spontaneously to larger particles at the micrometer scale or above. Green fluorescence from the Ab-conjugated nanospheres was observed by fluorescence microscopy. In contrast, no fluorescence was detected in the Ab-free nanospheres (Figure 2A and B). The fluorescence percentage detected by FCM analysis revealed that the antibody conjugation efficiency was 65.77% (Figure 3).

Entrapment efficiency and in vitro GEM release profiles

The encapsulation ratio of GEM detected by UV spectrophotometer was 82.16%. The curves of Figure 3 reveal how GEM was released in vitro from the C225-GEM/MANs. As indicated by the drug release pattern (Figure 4), GEM was

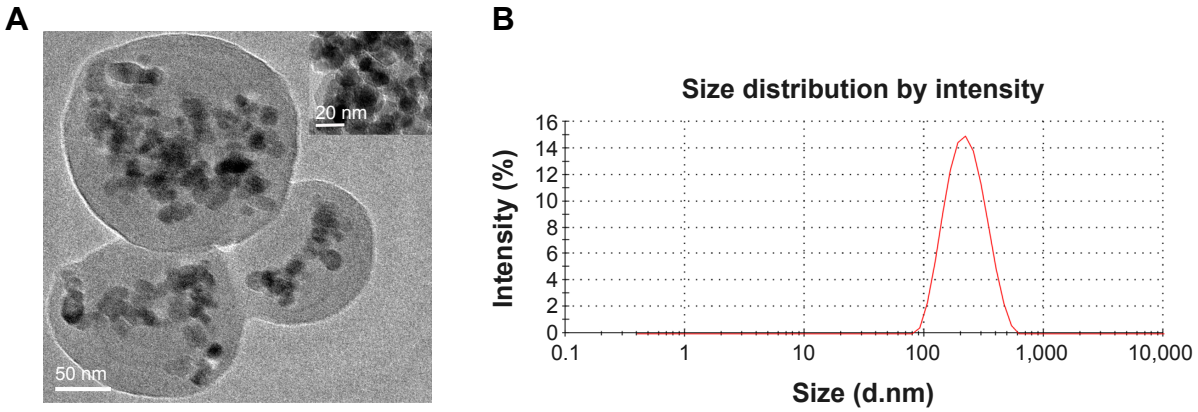

Figure 1 Characterization of C225-functionalized nanospheres containing nanosized Fe_3O_4 and GEM.
Notes: (**A**) The nanospheres were approximately spherical with a diameter of about 200 nm; Fe_3O_4 with a diameter of about 20 nm was successfully encapsulated into the nanospheres; (**B**) hydrodynamic diameter distribution of C225-GEM/MANs in PBS as measured by a particle size analyzer.
Abbreviations: C225, cetuximab; GEM, gemcitabine; PBS, phosphate-buffered saline; MANs, magnetic albumin nanospheres.

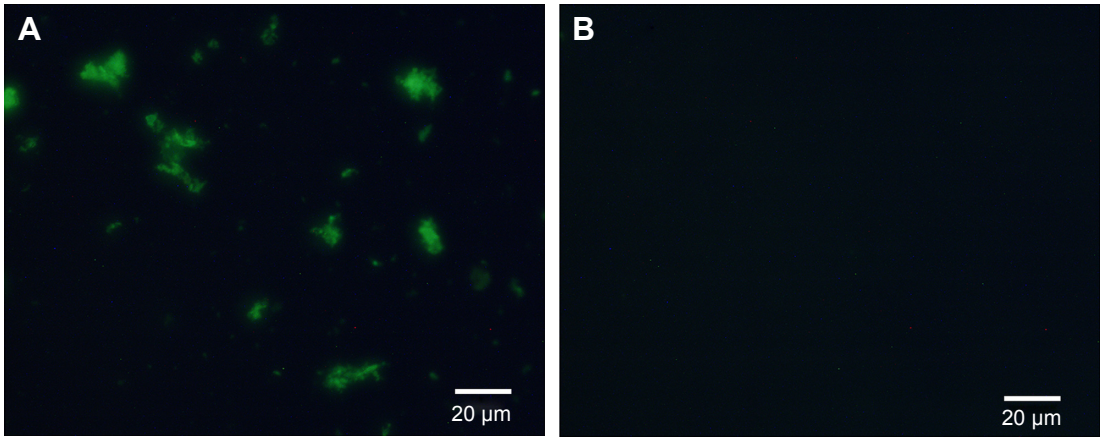

Figure 2 Determination of antibodies conjugated on the surface of the targeted nanospheres.
Notes: (**A**) The green fluorescence was seen in the C225-GEM/MANs; (**B**) no fluorescence could be detected in Ab-free nanospheres.
Abbreviations: C225, cetuximab; GEM, gemcitabine; MANs, magnetic albumin nanospheres.

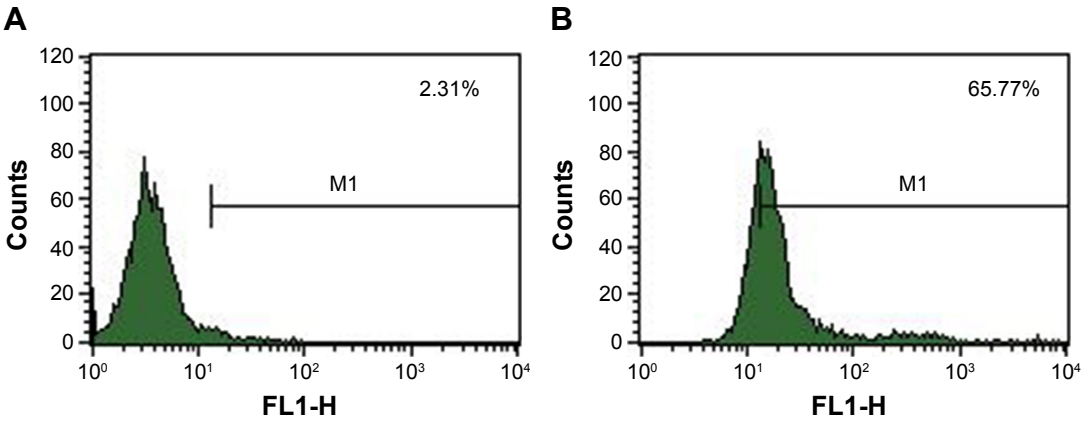

Figure 3 Determination of the antibody conjugation efficiency by measuring the fluorescence percentage.
Notes: (**A**) Fluorescence percentage of C225-GEM/MANs without incubation with FITC-labeled second antibody; (**B**) fluorescence percentage of C225-GEM/MANs after incubation with FITC-labeled second antibody.
Abbreviations: C225, cetuximab; FITC, fluorescein isothiocyanate; GEM, gemcitabine; MANs, magnetic albumin nanospheres.

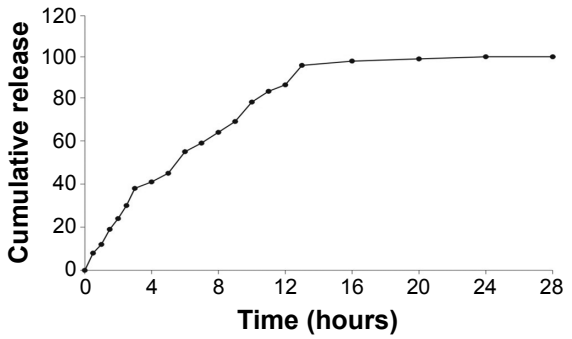

Figure 4 In vitro GEM release curve of the C225-GEM/MANs.
Note: The curve showed that GEM was released in vitro in a slow and steady manner until complete release after 24 hours.
Abbreviations: C225, cetuximab; GEM, gemcitabine; MANs, magnetic albumin nanospheres.

released in an explosive way in the first 30 minutes after administration, then gradually became slower.

The release lasted for nearly 12 hours and became steady. The pattern of drug liberation revealed that 20% of the drug was released within the first 2 hours, while 80% of the drug was released after 48 hours.

Temperature increase of the nanospheres in AMF

The iron content of the C225-GEM/MANs was 2.0 mg/mL. When varying concentrations of C225-GEM/MANs were exposed to a high-frequency alternating electromagnetic field, their temperature rose from 25°C to 55°C due to the heating effect of nanosized Fe_3O_4 (Figure 5). As the concentration increased, the maximum temperature rose. Among all of the tested concentrations, 0.24 mg/mL was the optimum. In the process of heating, the temperature rose quickly within the first 30 minutes, then rose gently, and stabilized at 4°C after 45 minutes. This hyperthermic behavior contributes to the killing of tumor cells while not harming normal tissues. The concentration of 0.24 mg/mL was selected to induce magnetic hyperthermia in the following experiment.

Targeted MRI in vitro

Due to the difference in cellular uptake of Fe_3O_4-containing nanospheres, different T2-weighted images were acquired (Figure 6A and B). Meanwhile, the T2 values corresponding to these images were also quantified (Figure 6C and D). As Figure 6A shows, after being incubated with C225-targeted nanospheres, the T2-weighted images of the AsPC-1 cells exhibited a significant MR signal reduction, while the T2-weighted imaging of MIA Paca2 cells demonstrated a mild signal reduction. The corresponding T2 value of the AsPC-1 cells was significantly different from that of the MIA Paca2 cells ($P<0.05$). When treated with C225-free nanospheres, the T2-weighted images of these two different types of pancreatic cells had a similarly weaker MR signal attenuation and they had similar T2 values ($P>0.05$). With regard to the differing cellular targeting effects, the MR T2 signal intensity in the combined magnetic- and antibody-targeted group decreased significantly, whereas a similar signal reduction was found in the C225-targeted alone and magnetic-targeted alone groups (Figure 6B). The T2 values of the targeted groups were significantly different from that of nontargeted group ($P<0.05$).

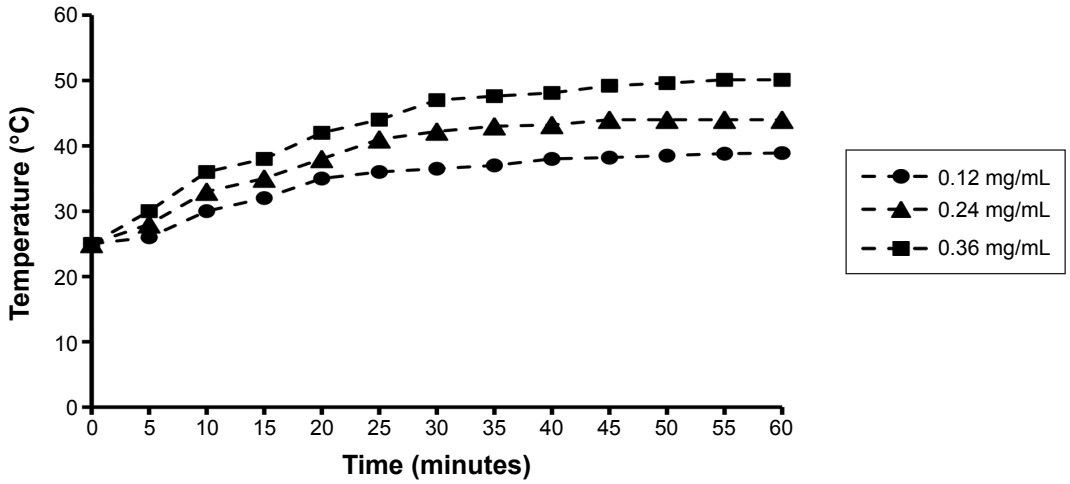

Figure 5 Heating curve for different concentrations of C225-GEM/MANs.
Notes: Under a high-frequency AMF (f=20 kHz; I=20 A), the targeted nanospheres at different concentrations rapidly reached the temperature required for thermochemotherapy (41°C–44°C) within 45 minutes, which remained stable after 15 minutes.
Abbreviations: AMF, alternating magnetic field; C225, cetuximab; GEM, gemcitabine; MANs, magnetic albumin nanospheres.

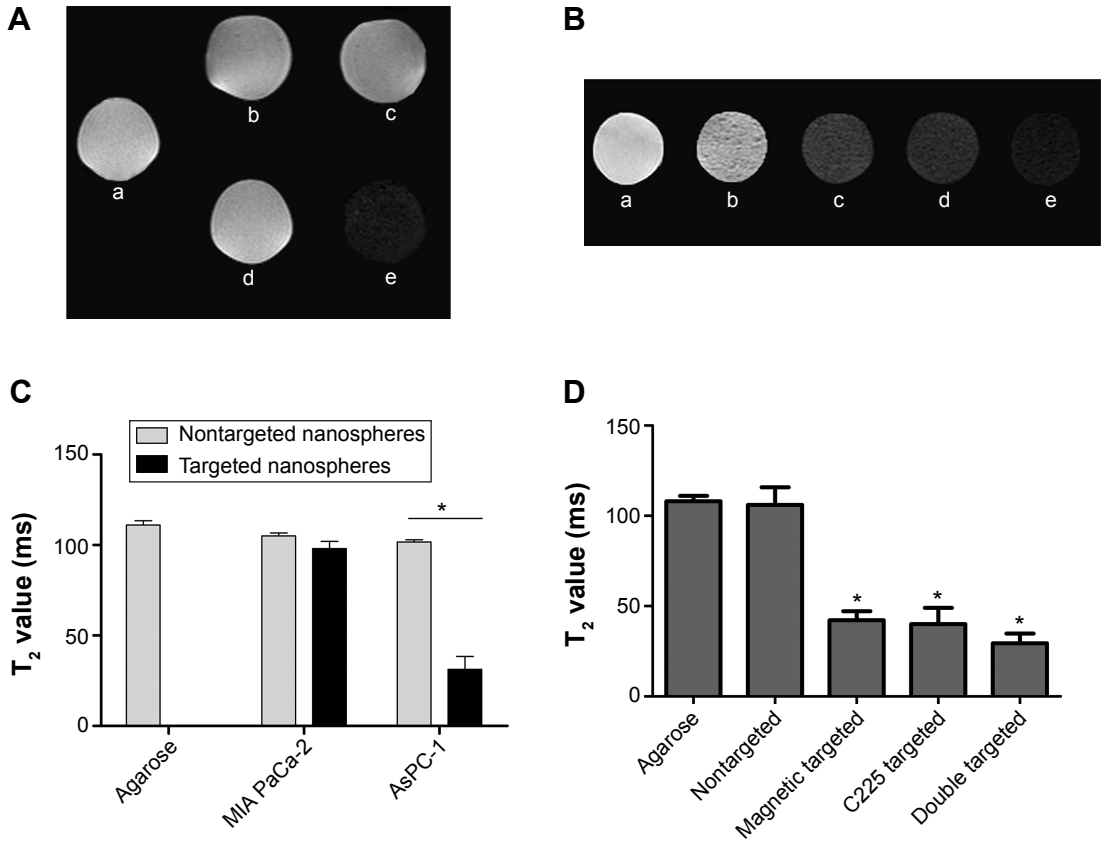

Figure 6 In vitro MRI.
Notes: (**A**) (a) Agarose gel without nanospheres; (b) MIA PaCa-2 cells incubated with untargeted nanospheres; (c) AsPC-1 cells incubated with untargeted nanospheres; (d) MIA PaCa-2 cells incubated with targeted nanospheres; and (e) AsPC-1 cells incubated with targeted nanospheres. (**B**) (a) Agarose gel without nanospheres; (b) AsPC-1 cells incubated with untargeted nanospheres; (c) AsPC-1 cells incubated with untargeted nanospheres with magnetic targeting; (d) AsPC-1 cells incubated with C225-conjugated nanospheres; and (e) AsPC-1 cells incubated with C225-conjugated nanospheres with magnetic targeting. (**C**) and (**D**) T2 values correspond to T2-weighted images of (**A**) and (**B**). Data are presented as the mean ± standard deviation, *$P<0.05$.
Abbreviations: C225, cetuximab; MRI, magnetic resonance imaging.

Increased uptake of C225-conjugated nanospheres in EGFR-overexpressing cell lines

C225-targeted nanospheres, nontargeted nanospheres, and C225 were incubated with AsPC-1 cells. As indicated by the intensity of the immunofluorescence (Figure 7A–D), C225 bound to AsPC-1 cells better than the other groups and showed strong green fluorescence. Compared to the C225 group, C225-targeted nanospheres also bound to cells, but showed less green fluorescence. There was hardly any binding fluorescence in the nontargeted group (Figure 7C) and the negative contrast group (Figure 7D).

The therapeutic effects on AsPC-1 cells

The average inhibitory rate of the thermochemotherapy groups was 58.50%, while the rate for the chemotherapy-alone groups was 47.50%.The mean apoptotic rates of the two therapy groups were 29.33% and 19.12%, respectively. The inhibition and apoptotic rates suggest that chemotherapy combined with MFH upon AFM has higher antitumor effects against AsPC-1 cells than chemotherapy ($P<0.05$, Figure 8A and B). For thermochemotherapy groups, the cell proliferation inhibition and apoptotic rates were 85.18% and 49.31%, respectively in the double-targeted thermochemotherapy group; 70.92% and 34.35%, respectively in the C225-targeted alone group; 46.95% and 20.10%, respectively in the magnetic-targeted alone group; and 30.97% and 13.56%, respectively in the nontargeted group. For the chemotherapy groups, the IRs were 75.89%, 55.86%, 39.96%, and 18.30% in the combined magnetic- and C225-targeted group, the C225-targeted group, the magnetic-targeted group, and the nontargeted group, respectively. The corresponding apoptotic indices for the four chemotherapy groups were 32.99%, 24.91%, 11.84%, and 6.72%, respectively. It was obvious that the therapeutic efficiency was higher in the targeted groups than in the nontargeted group. On the other hand,

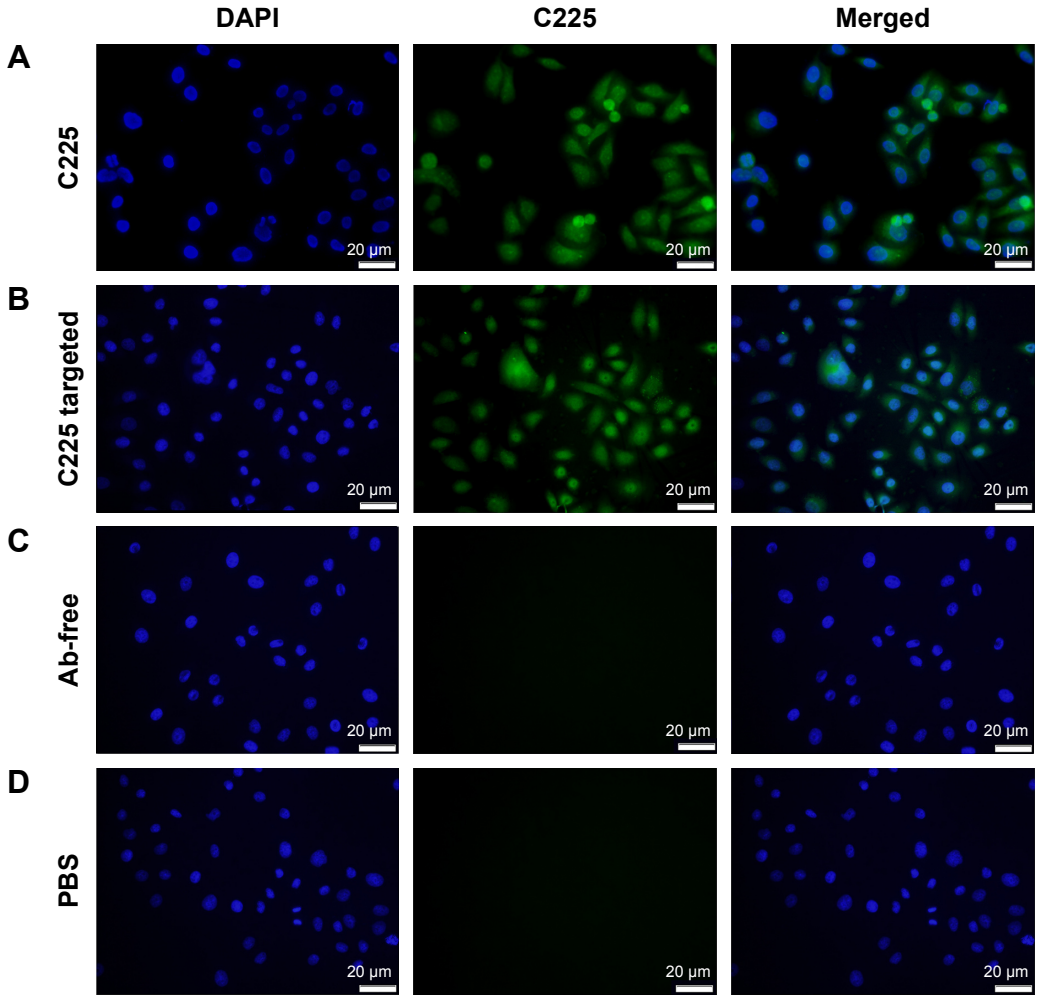

Figure 7 The specific interaction between AsPC-1 cells and C225-GEM/MANs.
Notes: AsPC-1 cells treated with (**A**) C225, showing strong green fluorescence; (**B**) C225-conjugated nanospheres, showing weaker green fluorescence; (**C**) nontargeted nanospheres; (**D**) PBS, showing no fluorescence.
Abbreviations: C225, cetuximab; DAPI, diamidino-2-phenylindole; GEM, gemcitabine; MANs, magnetic albumin nanospheres; PBS, phosphate-buffered saline.

despite thermochemotherapy or chemotherapy, double-targeted groups showed higher efficacy in inhibiting cell proliferation and inducing cell apoptosis. The double-targeted thermochemotherapy group achieved the best results among all the groups ($P<0.05$; Figure 8C–E).

Discussion

In this study, we successfully constructed multifunctional composite albumin nanospheres (named C225-GEM/MANs), which had a core–shell structure (Figure 9). Albumin served as the outer shells, while the interior core comprised Fe_3O_4 MNPs together with the antitumor drug GEM. Anti-EGFR mab C225 was further functionalized onto the surface of the nanospheres as the active targeted agent. With such a structure, a double-targeted multifunctional nanocarrier combining imaging and therapeutic capabilities was developed, capable of simultaneous diagnosis and thermochemotherapy of pancreatic cancer.

Our study found an over 80% GEM encapsulation rate and a sustained and steady drug-release profile, indicating that GEM as the first-line drug against pancreatic cancer had been successfully incorporated into the C225-modified nanospheres. Further, targeted nanospheres have also been proved to be effective drug delivery carriers. Similar to previous studies,[37,38] we also entrapped nanosized Fe_3O_4 with the aim of serving as an MRI contrast enhancement agent to noninvasively observe cellular uptake of Fe_3O_4 and antitumor drugs. Different targeted MRI of AsPC-1 and MIA PaCa-2 cells showed varying intakes of the targeted nanospheres, which corresponded with different expressions of EGFR. After being treated with targeted and nontargeted nanospheres, greater reductions in the T2

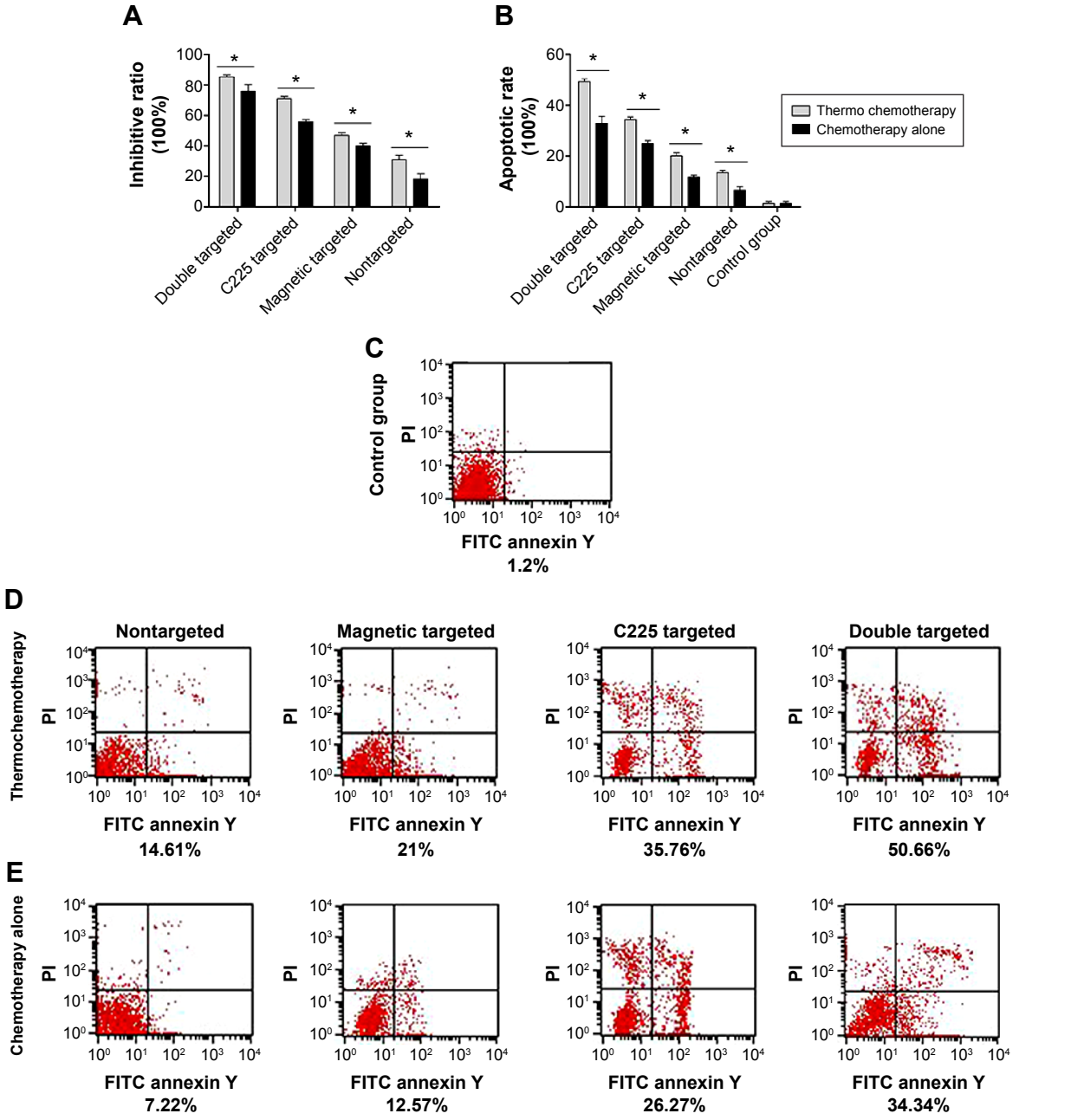

Figure 8 (**A**) Inhibition and (**B**) apoptotic rates of thermochemotherapy and chemotherapy-alone groups with different targeting methods against AsPC-1 cells. Data are presented as the mean ± standard deviation, *$P<0.05$. (**C**) Graphs of flow cytometry for untreated cells, (**D**) thermochemotherapy groups, and (**E**) chemotherapy-alone groups.
Abbreviations: FITC, fluorescein isothiocyanate; C225, cetuximab.

signal revealed that AsPC-1 was a high EGFR-expressing cell line, whereas MIA PaCa-2 belongs to a weak expressing cell line. This corresponded well with confirmatory western blot results.[33] These findings also suggested that C225-GEM/MANs can be applied as magnetic nanoprobes to noninvasively diagnosis early EGFR-positive pancreatic cancer via MRI. Additionally, the specific binding between AsPC-1 cells and C225-GEM/MANs was reflected through the presence of intense fluorescence in AsPC-1 cells treated with C225-targeted nanospheres and the absence of such fluorescence in cells treated with nontargeted counterparts. In addition, using targeted nanospheres as a noninvasive contrast agent to observe versatile targeted delivery effects on AsPC-1 cells also revealed good imaging effects. More obvious T2 signal reduction was found in cells treated with targeted nanospheres in a combined magnetic- and C225 mab-targeted manner. This demonstrated that double targeting can induce a higher cellular uptake of nanospheres and co-deliver a higher content of GEM and nanosized Fe_3O_4 into target cells. Thus, double targeting was confirmed to

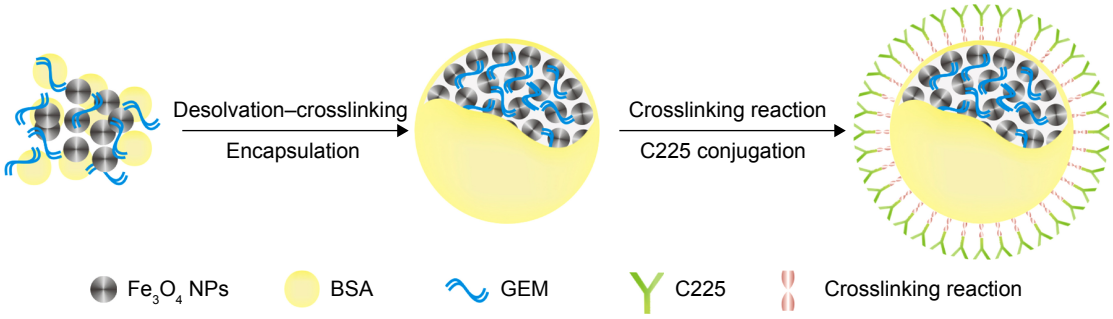

Figure 9 Schematic procedure for synthesis of C225-GEM/MANs.
Abbreviations: BSA, bovine serum albumin; C225, cetuximab; GEM, gemcitabine; MANs, magnetic albumin nanospheres; NPs, nanoparticles.

be an efficient approach, exhibiting better in vitro targeted therapeutic treatment.

Cancer is one of the most devastating diseases; single modality treatments are limited and not able to cure cancer alone. Studies in recent years have showed that multimodal therapy always exhibits more effectiveness in tumor suppression than single-modality treatment.[39–41] Thermochemotherapy for tumor therapy has attracted further attention and been widely used throughout the world, achieving satisfactory therapeutic outcomes.[42] In our study, we found that with either the targeted or nontargeted approaches, thermochemotherapy brought more significant inhibition of growth and induction of apoptosis in AsPC-1 cells than their chemotherapy-alone counterparts. Furthermore, the effect of double-targeted thermochemotherapy was the most significant. These results were in agreement with the MRI of cellular targeting effects, indicating that more GEM together with nanosized Fe_3O_4 was taken into cells owing to targeted co-delivery, especially in C225 targeting combined with magnetic targeting. Moreover, consistent with our previous findings reported by Li et al[34] combined thermochemotherapy mediated the highest rate of death of AsPC-1 cells compared to that of chemotherapy alone. Among all groups, the double-targeted thermochemotherapy group displayed the highest antitumor efficiency. The reason may be that the combination of magnetohyperthermia and chemotherapy is superior to any of them alone and hyperthermia makes tumor cells susceptible to chemotherapy.[43] On the other hand, C225- and magnetic-combined targeting can bring more enhanced targeted effects than single antibody targeting or magnetic targeting. The most important reason is that C225 mab can simultaneously serve as a therapeutic agent as well as a targeting agent. All of these findings highlighted the importance of double-targeted magnetohyperthermia in conjunction with chemotherapy against pancreatic cancer.

Cancer theranostics, which integrate therapeutic and diagnostic imaging functionalities, can be used for simultaneous imaging and treatment of cancers. Theranostic nanomedicine provides a promising nanoplatform for cancer theranostics.[44,45] Studies in recent years have shown that theranostics provide an attractive avenue for the detection and treatment of many tumors.[46–48] Our study also addressed a novel theranostic approach using a C225-conjugated nanocomposite for the simultaneously detection and chemohyperthermia co-therapy of pancreatic cancer. The nanocomplex presented here integrated targeting, diagnosis, and thermochemotherapy all within the same nanostructure. In this context, using C225-GEM/MANs as a diagnostic magnetic probe, two kinds of pancreatic cancer cells with different EGFR expression levels were well distinguished. Additionally, by C225-GEM/MANs mediating, combined antibody- and magnetic-targeted thermochemotherapy yielded an enhanced synergistic antitumor effect. As a result, the resultant C225-GEM/MANs exhibited great potential in multimodal theranostics, including active targeting, magnetic targeting, MRI diagnosis, drug delivery, and magnetohyperthermia, which provided a promising strategy for clinical therapeutic intervention for pancreatic cancer.

However, there are some limitations in our present work. All our therapeutic studies were at the in vitro level; more experiments in vivo should be tested in future research to further confirm the effect of double thermochemotherapy induced by C225-GEM/MANs against pancreatic cancers. Similarly, we conducted experiments only in in vitro cell MRI, while real-time evaluation of the in vivo targeting of drug delivery with noninvasive MRI scans needs to be elaborated further. Our study only used two EGFR-positive human pancreatic cancer cell lines (AsPC-1 and MIA PaCa-2) as model cells. Future research should include a wider spectrum of pancreatic cancer cell lines with various EGFR expression statuses to comprehensively explore the efficiency of double-targeted imaging and therapy.

In conclusion, we successfully synthesized C225-functionalized and GEM-loaded MANs. Our results confirm that the prepared C225-GEM/MANs can act as a diagnostic magnetic probe to effectively distinguish different EGFR-expressing pancreatic cancer cells and a noninvasive approach to evaluate different targeting effects by targeted MRI imaging. They can also be used as a double-targeted chemohyperthermic approach to achieve high intratumoral drug concentrations under combined antibody and magnetic targeting with the aid of an external magnetic field and permitting concurrent hyperthermia for more effective tumor cell killing and growth inhibition. Therefore, C225-GEM/MANs present a promising potential in multimodal theranostics of pancreatic cancer.

Disclosure

The authors report no conflicts of interest in this work.

References

1. Siegel R, Naishadham D, Jemal A. Cancer statistics, 2012. *CA: Cancer J Clin.* 2012;62(1):10–29.
2. Jemal A, Bray F, Center MM, et al. Global cancer statistics. *CA: Cancer J Clin.* 2011;61(2):69–90.
3. Paolino D, Cosco D, Racanicchi L, et al. Gemcitabine-loaded PEGylated unilamellar liposomes vs GEMZAR: biodistribution, pharmacokinetic features and in vivo antitumor activity. *J Control Release.* 2010;144(2):144–150.
4. Zhou J, Wang J, Xu Q, et al. Folate-chitosan-gemcitabine core-shell nanoparticles targeted to pancreatic cancer. *Chin J Cancer Res.* 2013; 25(5):527–535.
5. Vittorio O, Voliani V, Faraci P, et al. Magnetic catechin-dextran conjugate as targeted therapeutic for pancreatic tumour cells. *J Drug Target.* 2014;22(5):408–415.
6. Sim H, Bibee K, Wickline S, et al. Pharmacokinetic modeling of tumor bioluminescence implicates efflux, and not influx, as the bigger hurdle in cancer drug therapy. *Cancer Res.* 2011;71(3):686–692.
7. Chen W, Ayala-Orozco C, Biswal NC, et al. Targeting pancreatic cancer with magneto-fluorescent theranostic gold nanoshells. *Nanomedicine (Lond).* 2014;9(8):1209–1222.
8. Schleich N, Sibret P, Danhier P, et al. Dual anticancer drug/superparamagnetic iron oxide-loaded PLGA-based nanoparticles for cancer therapy and magnetic resonance imaging. *Int J Pharm.* 2013;447(1–2):94–101.
9. Ao L, Wang B, Liu P, et al. A folate-integrated magnetic polymer micelle for MRI and dual targeted drug delivery. *Nanoscale.* 2014; 6(18):10710–10716.
10. Deng WJ, Yang XQ, Liang YJ, et al. FG020326-loaded nanoparticle with PEG and PDLLA improved pharmacodynamics of reversing multidrug resistance in vitro and in vivo. *Acta Pharmacol Sin.* 2007; 28(6):913–920.
11. Meng XX, Wan JQ, Jing M, et al. Specific targeting of gliomas with multifunctional superparamagnetic iron oxide nanoparticle optical and magnetic resonance imaging contrast agents. *Acta Pharmacol Sin.* 2007;28(12):2019–2026.
12. Elzoghby AO, Samy WM, Elgindy NA. Albumin-based nanoparticles as potential controlled release drug delivery systems. *J Control Release.* 2012;157(2):168–182.
13. Ak G, Yılmaz H, Sanlıer SH. Preparation of magnetically responsive albumin nanospheres and in vitro drug release studies. *Artif Cells Nanomed Biotechnol.* 2014;42(1):18–26.
14. Li J, Di Y, Jin C, et al. Gemcitabine-loaded albumin nanospheres (GEM-ANPs) inhibit PANC-1 cells in vitro and in vivo. *Nanoscale Res Lett.* 2013;8(1):176.
15. Li JM, Chen W, Wang H, et al. Preparation of albumin nanospheres loaded with gemcitabine and their cytotoxicity against BXPC-3 cells in vitro. *Acta Pharmacol Sin.* 2009;30(9):1337–1343.
16. Jia Y, Yuan M, Yuan H, et al. Co-encapsulation of magnetic Fe3O4 nanoparticles and doxorubicin into biodegradable PLGA nanocarriers for intratumoral drug delivery. *Int J Nanomedicine.* 2012;7: 1697–1708.
17. Latorre M, Rinaldi C. Applications of magnetic nanoparticles in medicine: magnetic fluid hyperthermia. *P R Health Sci J.* 2009; 28(3):227–238.
18. Chen YC, Wen S, Shang SA, Cui Y, Luo B, Teng GJ. Magnetic resonance and near-infrared imaging using a novel dual-modality nano-probe for dendritic cell tracking in vivo. *Cytotherapy.* 2014; 16(5):699–710.
19. Yuan C, An Y, Zhang J, et al. Magnetic nanoparticles for targeted therapeutic gene delivery and magnetic-inducing heating on hepatoma. *Nanotechnology.* 2014;25(34):345101.
20. Tietze R, Lyer S, Durr S, et al. Nanoparticles for cancer therapy using magnetic forces. *Nanomedicine (Lond).* 2012;7(3):447–457.
21. Zeybek A, Şanlı-Mohamed G, Ak G, Yılmaz H, Şanlıer ŞH. In vitro evaluation of doxorubicin-incorporated magnetic albumin nanospheres. *Chem Biol Drug Des.* 2014;84(1):108–115.
22. Yang R, An Y, Miao F, Li M, Liu P, Tang Q. Preparation of folic acid-conjugated, doxorubicin-loaded, magnetic bovine serum albumin nanospheres and their antitumor effects in vitro and in vivo. *Int J Nanomedicine.* 2014;9:1–13.
23. Yang R, Chen D, Li M, Miao F, Liu P, Tang Q. 20(s)-ginsenoside Rg3-loaded magnetic human serum albumin nanospheres applied to HeLa cervical cancer cells in vitro. *Biomed Mater Eng.* 2014; 24(6):1991–1998.
24. Portilho FA, Estevanato LL, Miranda-Vilela AL, et al. Investigation of a magnetohyperthermia system efficacy. *J Appl Phys.* 2011; 109:07B307.
25. Tang Q, An Y, Liu D, Liu P, Zhang D. Folate/NIR 797-conjugated albumin magnetic nanospheres: synthesis, characterisation, and in vitro and in vivo targeting evaluation. *PLoS One.* 2014;9(9):e106483.
26. Shen Z, Li Y, Kohama K, Oneill B, Bi J. Improved drug targeting of cancer cells by utilizing actively targetable folic acid-conjugated albumin nanospheres. *Pharmacol Res.* 2011;63(1):51–58.
27. Bloomston M, Bhardwaj A, Ellison EC, Frankel WL. Epidermal growth factor receptor expression in pancreatic carcinoma using tissue microarray technique. *Dig Surg.* 2006;23(1–2):74–79.
28. Xiong HQ, Rosenberg A, LoBuglio A, et al. Cetuximab, a monoclonal antibody targeting the epidermal growth factor receptor, in combination with gemcitabine for advanced pancreatic cancer: a multicenter phase II trial. *J Clin Oncol.* 2004;22(13):2610–2616.
29. Baselga J. Why the epidermal growth factor receptor? The rationale for cancer therapy. *Oncologist.* 2002;7 Suppl 4:2–8.
30. Moore MJ, Goldstein D, Hamm J, et al; National Cancer Institute of Canada Clinical Trials Group. Erlotinib plus gemcitabine compared with gemcitabine alone in patients with advanced pancreatic cancer: a phase III trial of the National Cancer Institute of Canada Clinical Trials Group. *J Clin Oncol.* 2007;25(15):1960–1966.
31. Rocha-Lima CM, Soares HP, Raez LE, Singal R. EGFR targeting of solid tumors. *Cancer Control.* 2007;14(3):295–304.
32. Owonikoko TK, Sun SY, Ramalingam SS. The role of cetuximab in the management of non-small-cell lung cancer. *Clin Lung Cancer.* 2009; 10(4):230–238.
33. Patra CR, Bhattacharya R, Wang EF, et al. Targeted delivery of gemcitabine to pancreatic adenocarcinoma using cetuximab as a targeting agent. *Cancer Res.* 2008;68(6):1970–1978.
34. Li H, Ke F, An Y, et al. Gemcitabine-loaded magnetic albumin nanospheres for cancer chemohyperthermia. *J Nanopart Res.* 2013;15: 1513.

35. Du Y, Zhang D, Liu H, Lai R. Thermochemotherapy effect of nanosized As2O3/Fe3O4 complex on experimental mouse tumors and its influence on the expression of CD44v6, VEGF-C and MMP-9. *BMC Biotechnol.* 2009;9:84.
36. Liu D, Wu W, Ling J, et al. Effective PEGylation of iron oxide nanoparticles for high performance in vivo cancer imaging. *Adv Funct Mater.* 2011;21(8):1498–1504.
37. Li J, An YL, Zang FC, Zong SF, Cui YP, Teng GJ. A dual mode targeting probe for distinguishing HER2-positive breast cancer cells using silica-coated fluorescent magnetic nanoparticles. *J Nanopart Res.* 2013;15:1980.
38. Zhang L, Gong FM, Zhang F, Ma J, Zhang P, Shen J. Targeted therapy for human hepatic carcinoma cells using folate-functionalized polymeric micelles loaded with superparamagnetic iron oxide and sorafenib in vitro. *Int J Nanomedicine.* 2013;8:1517–1524.
39. Kheirolomoom A, Lai CY, Tam SM, et al. Complete regression of local cancer using temperature-sensitive liposomes combined with ultrasound-mediated hyperthermia. *J Control Release.* 2013;172(1):266–273.
40. Zheng M, Yue C, Ma Y, et al. Single-step assembly of DOX/ICG loaded lipid – polymer nanoparticles for highly effective chemo-photothermal combination therapy. *ACS Nano.* 2013;7(3):2056–2067.
41. Mi Y, Guo YJ, Feng SS. Nanomedicine for multimodality treatment of cancer. *Nanomedicine (Lond).* 2012;7(12):1791–1794.
42. McQuellon RP, Russell GB, Shen P, et al. Survival and health outcomes after cytoreductive surgery with intraperitoneal hyperthermic chemotherapy for disseminated peritoneal cancer of appendiceal origin. *Ann Surg Oncol.* 2008;15(1):125–133.
43. Rao W, Deng ZS, Liu J. A review of hyperthermia combined with radiotherapy/chemotherapy on malignant tumors. *Crit Rev Biomed Eng.* 2010;38(1):101–116.
44. Min KH, Min HS, Lee HJ, et al. pH-controlled gas-generating mineralized nanoparticles: a theranostic agent for ultrasound imaging and therapy of cancers. *ACS Nano.* 2015;9(1):134–145.
45. Rhee JK, Park OK, Lee A, Yang DH, Park K. Glycol chitosan-based fluorescent theranostic nanoagents for cancer therapy. *Marine Drugs.* 2014;12(12):6038–6057.
46. Peng J, Qi T, Liao J, et al. Mesoporous magnetic gold "nanoclusters" as theranostic carrier for chemo-photothermal co-therapy of breast cancer. *Theranostics.* 2014;4(7):678–692.
47. Alberti D, Protti N, Toppino A, et al. A theranostic approach based on the use of a dual boron/Gd agent to improve the efficacy of Boron Neutron Capture Therapy in the lung cancer treatment. *Nanomedicine (Lond).* Epub 2015 Jan 14.
48. Dixit S, Novak T, Miller K, Zhu Y, Kenney ME, Broome AM. Transferrin receptor-targeted theranostic gold nanoparticles for photosensitizer delivery in brain tumors. *Nanoscale.* 2015;7(5):1782–1790.